

CONSTRAINTS TO DARK ENERGY USING PADE PARAMETERISATIONS

M. REZAEI¹, M. MALEKJANI¹, S. BASILAKOS², A. MEHRABI¹, AND D. F. MOTA³

¹ Department of Physics, Bu-Ali Sina University, Hamedan 65178, Iran

²Academy of Athens, Research Center for Astronomy and Applied Mathematics, Soranou Efessiou 4, 11-527 Athens, Greece
and

³Institute of Theoretical Astrophysics, University of Oslo, 0315 Oslo, Norway

Abstract

We put constraints on dark energy properties using the PADE parameterisation, and compare it to the same constraints using Chevalier-Polarski-Linder (CPL) and Λ CDM, at both the background and the perturbation levels. The dark energy equation of state parameter of the models is derived following the mathematical treatment of PADE expansion. Unlike CPL parameterisation, the PADE approximation provides different forms of the equation of state parameter which avoid the divergence in the far future. Initially, we perform a likelihood analysis in order to put constraints on the model parameters using solely background expansion data and we find that all parameterisations are consistent with each other. Then, combining the expansion and the growth rate data we test the viability of PADE parameterisations and compare them with CPL and Λ CDM models respectively. Specifically, we find that the growth rate of the current PADE parameterisations is lower than Λ CDM model at low redshifts, while the differences among the models are negligible at high redshifts. In this context, we provide for the first time growth index of linear matter perturbations in PADE cosmologies. Considering that dark energy is homogeneous we recover the well known asymptotic value of the growth index, namely $\gamma_\infty = \frac{3(w_\infty - 1)}{6w_\infty - 5}$, while in the case of clustered dark energy we obtain $\gamma_\infty \simeq \frac{3w_\infty(3w_\infty - 5)}{(6w_\infty - 5)(3w_\infty - 1)}$. Finally, we generalize the growth index analysis in the case where γ is allowed to vary with redshift and we find that the form of $\gamma(z)$ in PADE parameterisation extends that of the CPL and Λ CDM cosmologies respectively.

1. INTRODUCTION

Various independent cosmic observations including those of type Ia supernova (SnIa) (Riess et al. 1998; Perlmutter et al. 1999; Kowalski et al. 2008), cosmic microwave background (CMB) (Komatsu et al. 2009; Jarosik et al. 2011; Komatsu et al. 2011; Planck Collaboration XIV 2016), large scale structure (LSS), baryonic acoustic oscillation (BAO) (Tegmark et al. 2004; Cole et al. 2005; Eisenstein et al. 2005; Percival et al. 2010; Blake et al. 2011b; Reid et al. 2012), high redshift galaxies (Alcaniz 2004), high redshift galaxy clusters (Wang & Steinhardt 1998a; Allen et al. 2004) and weak gravitational lensing (Benjamin et al. 2007; Amendola et al. 2008; Fu et al. 2008) reveal that the present universe experiences an accelerated expansion. Within the framework of General Relativity (GR), the physical origin of the cosmic acceleration can be described by invoking the existence of an exotic fluid with sufficiently negative pressure, the so-called Dark Energy (DE). One possibility is that DE consists of the vacuum energy or cosmological constant Λ with constant EoS parameter $w_\Lambda = -1$ (Peebles & Ratra 2003). Alternatively, the fine-tuning and cosmic coincidence

problems (Weinberg 1989; Sahni & Starobinsky 2000; Carroll 2001; Padmanabhan 2003; Copeland et al. 2006) led the scientific community to suggest a time evolving energy density with negative pressure. In those models, the EoS parameter is a function of redshift, $w(z)$ (Caldwell et al. 1998; Erickson et al. 2002; Armendariz-Picon et al. 2001; Caldwell 2002; Padmanabhan 2002; Elizalde et al. 2004). A precise measurement of EoS parameter and its variation with cosmic time can provide important clues about the dynamical behavior of DE and its nature (Copeland et al. 2006; Frieman et al. 2008; Weinberg et al. 2013; Amendola et al. 2013).

One possible way to study the EoS parameter of dynamical DE models is via a parameterisation. In literature, one can find many different EoS parameterisations. One of the simplest and earliest parameterisations is the Taylor expansion of $w_{\text{de}}(z)$ with respect to redshift z up to first order as: $w_{\text{de}}(z) = w_0 + w_1 z$ (Maor et al. 2001; Riess et al. 2004). It can also be generalized by considering the second order approximation in Taylor series as: $w_{\text{de}}(z) = w_0 + w_1 z + w_2 z^2$ (Bassett et al. 2008). However, these two parameterisations diverge at high redshifts. Hence the

well-known Chevallier-Polarski-Linder (CPL) parameterisation, $w_{\text{de}}(z) = w_0 + w_1(1 - a) = w_0 + w_1z/(1 + z)$, was proposed (Chevallier & Polarski 2001; Linder 2003). The CPL parameterisation can be considered as a Taylor series with respect to $(1 - a)$ and was extended to more general case by assuming the second order approximation as: $w_{\text{de}}(a) = w_0 + w_1(1 - a) + w_2(1 - a)^2$ (Seljak et al. 2005). In addition to CPL formula, some purely phenomenological parameterisations have been proposed more recently. For example $w_{\text{de}}(z) = w_0 + w_1z/(1 + z)^\alpha$, where α is fixed to 2 (Jassal et al. 2005). In this class, the power law $w_{\text{de}}(a) = w_0 + w_1(1 - a^\beta)/\beta$ (Barboza et al. 2009) and logarithmic $w_{\text{de}}(a) = w_0 + w_1 \ln a$ (Efstathiou 1999) parameterisations have been investigated. Another logarithm parameterisation is $w_{\text{de}}(z) = w_0/[1 + b \ln(1 + z)]^\alpha$, where α is taken to be 1 or 2 (Wetterich 2004). Notice that although the CPL is a well-behaved parameterisation at early ($a \ll 1$) and present ($a \sim 1$) epochs, it diverges when the scale factor goes to infinity. This is also a common difficulty for the above phenomenological parameterisations. Recently to solve the divergence, several phenomenological parameterisations have been introduced (see Dent et al. 2009; Frampton & Ludwick 2011; Feng et al. 2012, for more details). Notice that most of these EoS parameterisations are *ad hoc* and purely written by hand where there is no mathematical principle or fundamental physics behind them. In this work we focus on the PADE parameterisation (see section 2), which from the mathematical point of view seems to be more stable: it does not diverge and can be employed at both small and high redshifts. Using the different types of PADE parameterisations to express the EoS parameter of DE w_{de} in terms of redshift z , we study the growth of perturbations in the universe.

DE not only accelerate the expansion rate of universe but also change the evolution of growth rate of matter perturbations and consequently the formation epochs of large scale structures of universe (Armendariz-Picon et al. 1999; Garriga & Mukhanov 1999; Armendariz-Picon et al. 2000; Tegmark et al. 2004; Pace et al. 2010; Akhoury et al. 2011). Moreover, the growth of cosmic structures are also affected by perturbations of DE when we deal with dynamical DE models with time varying EoS parameter $w_{\text{de}} \neq -1$ (Erickson et al. 2002; Bean & Doré 2004; Hu & Scranton 2004; Basilakos & Voglis 2007; Ballesteros & Riotto 2008; Basilakos et al. 2009a; Koivisto & Mota 2007; Mota et al. 2007; Gannouji et al. 2010; Basilakos et al. 2010; Sapone & Majerotto 2012; Batista & Pace 2013; Dossett & Ishak 2013; Basse et al. 2014; Pace et al. 2014c; Batista 2014; Basilakos 2015; Pace et al. 2014b; Nesseris & Sapone 2014; Mehrabi et al. 2015c,b; Malekjani et al. 2015; Mehrabi et al. 2015a; Malekjani et al. 2017).

In addition to the background geometrical data the data coming from the formation of large scale structures provide a valuable information about the nature of DE. In particular, we

can setup a more general formalism in which the background expansion data including SnIa, BAO, CMB shift parameter, Hubble expansion data joined with the growth rate data of large scale structures in order to put constraints on the parameters of cosmology and DE models (see Cooray et al. 2004; Corasaniti et al. 2005; Basilakos et al. 2010; Blake et al. 2011b; Nesseris et al. 2011; Basilakos & Pouri 2012; Yang et al. 2014; Koivisto & Mota 2007; Mota et al. 2007; Gannouji et al. 2010; Mota et al. 2008; Llinares et al. 2014; Llinares & Mota 2013; Contreras et al. 2013; Chuang et al. 2013; Li et al. 2014; Basilakos 2015; Mehrabi et al. 2015a,b; Basilakos 2016; Mota et al. 2010; Malekjani et al. 2017; Fay 2016; Bonilla Rivera & Farieta 2016).

In this work, following the lines of the above studies and using the latest observational data including the geometrical data set (SnIa, BAO, CMB, big bang nucleosynthesis (BBN), $H(z)$) combined with growth rate data $f(z)\sigma_8$, we perform an overall likelihood statistical analysis to place constraints and find best fit values of the cosmological parameters where the EoS parameter of DE is approximated by PADE parameterisations. Previously, the PADE parameterisations have been studied from different observational tests in Cosmology. For example in Gruber & Luongo (2014), the cosmography analysis has been investigated using the PADE approximation. In Wei et al. (2014), the authors proposed several parameterisations for EoS of DE on the basis of PADE approximation. Confronting these EoS parameterisations with the latest geometrical data, they found that the PADE parameterisations can work well (for similar studies, see Aviles et al. 2014; Zaninetti 2016; Zhou et al. 2016). Here, for the first time, we study the growth of perturbations in PADE cosmologies. After introducing the main ingredients of PADE parameterisations in Sect.2, we study the background evolution of the universe in Sect.(3). We implement the likelihood analysis using the geometrical data to put constraints on the cosmological and model parameters in PADE parameterisations. In Sect.(4), the growth of perturbations in PADE cosmologies is investigated. Then we perform an overall likelihood analysis including the geometrical + growth rate data to place constraints and obtain the best fit values of the corresponding cosmological parameters. Finally we provide the main conclusions in Sect.(5).

2. PADE PARAMETERISATIONS

For an arbitrary function $f(x)$, the PADE approximate of order (m, n) is given by the following rational function (Pade 1892; Baker & Graves-Morris 1996; Adachi & Kasai 2012)

$$f(x) = \frac{a_0 + a_1x + a_2x^2 + \dots + a_nx^n}{b_0 + b_1x + b_2x^2 + \dots + b_mx^m}, \quad (1)$$

where exponents (m, n) are positive and the coefficients (a_i, b_i) are constants. Obviously, for $b_i = 0$ (with $i \geq 1$) the current approximation reduces to standard Taylor expansion. In this study we focus on three PADE parameterisations

introduced as follows (see also [Wei et al. 2014](#)).

2.1. PADE (I)

Based on Eq. (1), we first expand the EoS parameter w_{de} with respect to $(1 - a)$ up to order (1, 1) as follows (see also [Wei et al. 2014](#)):

$$w_{\text{de}}(a) = \frac{w_0 + w_1(1 - a)}{1 + w_2(1 - a)}. \quad (2)$$

From now on we will call the above formula as PADE (I) parameterisation. In terms of redshift z , Eq. (2) is written as

$$w_{\text{de}}(z) = \frac{w_0 + (w_0 + w_1)z}{1 + (1 + w_2)z}. \quad (3)$$

As expected for $w_2 = 0$ Eq. (2) boils down to CPL parameterisation. Unlike CPL parameterisation, here the EoS parameter with $w_2 \neq 0$ avoids the divergence at $a \rightarrow \infty$ (or equivalently at $z = -1$). Using Eq. (2) we find the following special cases regarding the EoS parameter (see also [Wei et al. 2014](#))

$$w_{\text{de}} = \begin{cases} \frac{w_0 + w_1}{1 + w_2}, & \text{for } a \rightarrow 0 \text{ (} z \rightarrow \infty, \text{ early time),} \\ w_0, & \text{for } a = 1 \text{ (} z = 0, \text{ present),} \\ \frac{w_1}{w_2}, & \text{for } a \rightarrow \infty \text{ (} z \rightarrow -1, \text{ far future),} \end{cases} \quad (4)$$

where we need to set $w_2 \neq 0$ and -1 . Therefore, we argue that PADE (I) formula is a well-behaved function in the range of $0 \leq a \leq \infty$ (or equivalently at $-1 \leq z \leq \infty$).

2.2. simplified PADE (I)

Clearly, PADE (I) approximation has three free parameters w_0 , w_1 and w_2 . Setting $w_1 = 0$ we provide a simplified version of PADE (I) parameterisation, namely

$$w_{\text{de}}(a) = \frac{w_0}{1 + w_2(1 - a)}. \quad (5)$$

Notice, that in order to avoid singularities in the cosmic expansion w_2 needs to lie in the interval $-1 < w_2 < 0$.

2.3. PADE (II)

Unlike the previous cases, here the current parameterisation is written as a function of $N = \ln a$. In this context, the EoS parameter up to order (1, 1) takes the form

$$w_{\text{de}}(a) = \frac{w_0 + w_1 \ln a}{1 + w_2 \ln a}, \quad (6)$$

Table 1. The statistical results for the various DE parameterisations used in the analysis. These results are based on the expansion data. The concordance Λ CDM model is shown for comparison.

Model	PADE I	simp. PADE I	PADE II	CPL	Λ CDM
k	6	5	6	5	3
χ^2_{min}	567.6	567.7	567.9	567.6	574.4
AIC	579.6	577.7	579.9	577.6	580.4
BIC	606.1	599.8	606.4	599.7	593.6

where w_0 , w_1 and w_2 are constants (see also [Wei et al. 2014](#)). In PADE (II) parameterisation, we can easily show that

$$w_{\text{de}} = \begin{cases} \frac{w_1}{w_2}, & \text{for } a \rightarrow 0 \text{ (} z \rightarrow \infty, \text{ early time),} \\ w_0, & \text{for } a = 1 \text{ (} z = 0, \text{ present),} \\ \frac{w_1}{w_2}, & \text{for } a \rightarrow \infty \text{ (} z \rightarrow -1, \text{ far future),} \end{cases} \quad (7)$$

Notice, that in order to avoid singularities at the above epochs we need to impose $w_2 \neq 0$.

3. BACKGROUND HISTORY IN PADE PARAMETERISATIONS

In this section based on the aforementioned parameterisations we study the background evolution in PADE cosmologies. Generally speaking, for isotropic and homogeneous spatially flat FRW cosmologies, driven by radiation, non-relativistic matter and an exotic fluid with an equation of state $p_{\text{de}} = w_{\text{de}}\rho_{\text{de}}$, the first Friedmann equation reads

$$H^2 = \frac{8\pi G}{3}(\rho_r + \rho_m + \rho_{\text{de}}), \quad (8)$$

where $H \equiv \dot{a}/a$ is the Hubble parameter, ρ_r , ρ_m and ρ_{de} are the energy densities of radiation, dark matter and DE, respectively. In the absence of interactions among the three fluids the corresponding energy densities satisfy the following differential equations

$$\dot{\rho}_r + 4H\rho_r = 0, \quad (9)$$

$$\dot{\rho}_m + 3H\rho_m = 0, \quad (10)$$

$$\dot{\rho}_{\text{de}} + 3H(1 + w_{\text{de}})\rho_{\text{de}} = 0, \quad (11)$$

where the over-dot denotes a derivative with respect to cosmic time t . Based on Eqs. (9) and (10), it is easy to derive the evolution of radiation and pressure-less matter, namely $\rho_r = \rho_{r0}a^{-4}$ and $\rho_m = \rho_{m0}a^{-3}$. Inserting Eqs. (2), (5) and (6) into equation (11), we can obtain the DE density of the current PADE parameterisations (see also [Wei et al. 2014](#))

$$\begin{aligned} \rho_{\text{de}}^{(\text{PADEI})} &= \rho_{\text{de}}^{(0)} a^{-3\left(\frac{1+w_0+w_1+w_2}{1+w_2}\right)} [1 + w_2(1 - a)]^{-3\left(\frac{w_1 - w_0 w_2}{w_2(1+w_2)}\right)} \quad (12) \\ \rho_{\text{de}}^{(\text{simp.PADEI})} &= \rho_{\text{de}}^{(0)} a^{-3\left(\frac{1+w_0+w_2}{1+w_2}\right)} [1 + w_2(1 - a)]^{-3\left(\frac{-w_0 w_2}{w_2(1+w_2)}\right)} \quad (13) \\ \rho_{\text{de}}^{(\text{padeII})} &= \rho_{\text{de}}^0 a^{-3\left(\frac{w_1+w_2}{w_2}\right)} (1 + w_2 \ln a)^{3\left(\frac{w_1 - w_0 w_2}{w_2^2}\right)} \quad (14) \end{aligned}$$

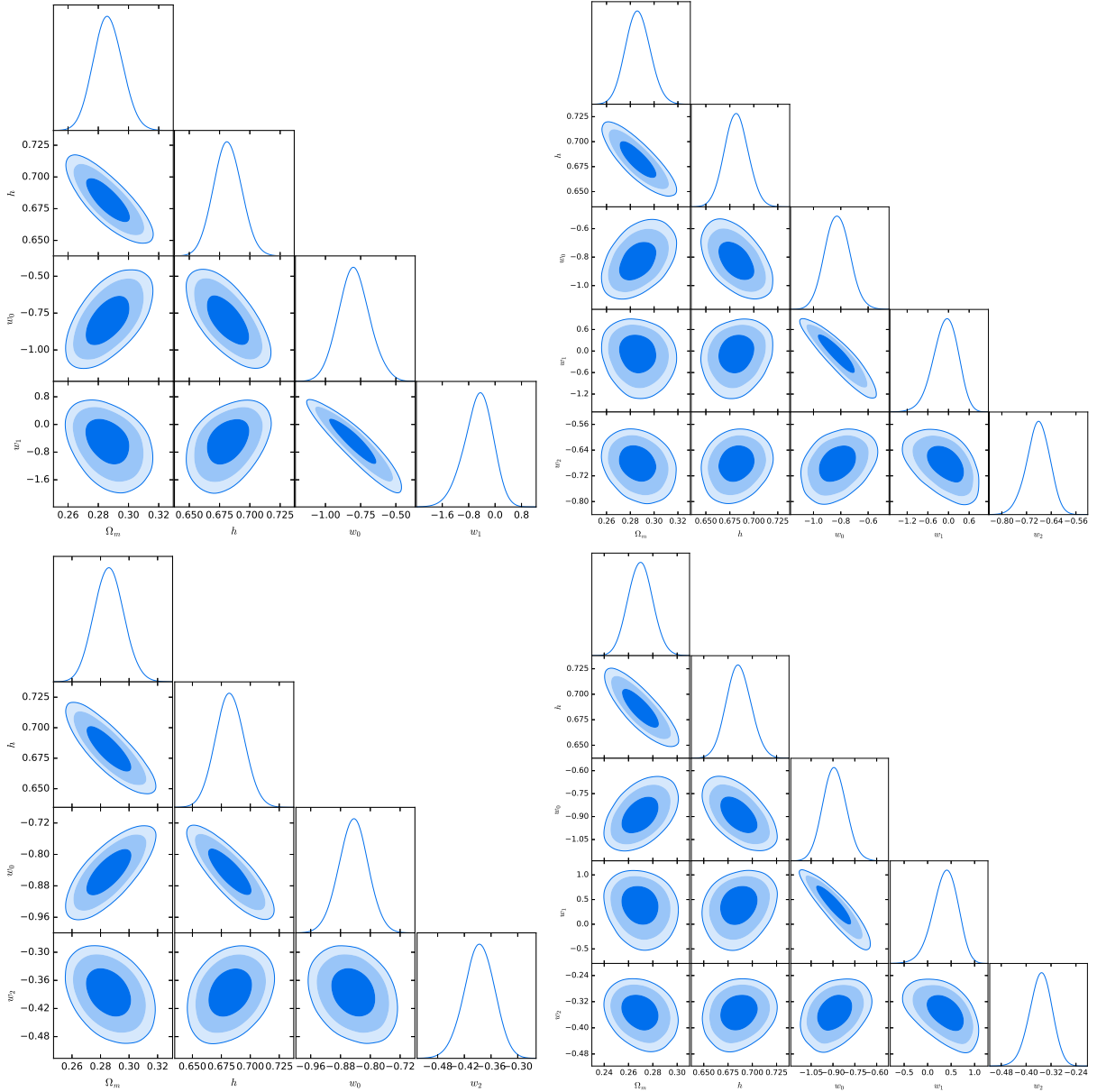


Figure 1. The 1σ , 2σ and 3σ likelihood contours for various cosmological parameters using the latest expansion data. The upper left (upper right) panel shows the results for CPL (PADE I) parameterisation. The lower left (lower right) panel shows the results for simplified PADE I (PADE II) parameterisation.

Also, combining Eqs.(12, 13, 14) and Eq.(8) we derive the dimensionless Hubble parameter $E = H/H_0$ (see also Wei et al. 2014). Specifically, we find

$$E_{\text{PADEI}}^2 = \Omega_{r0}a^{-4} + \Omega_{m0}a^{-3} + (1 - [\Omega_{r0} + \Omega_{m0}]) \times a^{-3\left(\frac{1+w_0+w_1+w_2}{1+w_2}\right)} \times (1 + w_2 - aw_2)^{-3\left(\frac{w_1-w_0w_2}{w_2(1+w_2)}\right)}, \quad (15)$$

$$E_{\text{simPADEI}}^2 = \Omega_{r0}a^{-4} + \Omega_{m0}a^{-3} + (1 - [\Omega_{r0} + \Omega_{m0}]) \times a^{-3\left(\frac{1+w_0+w_2}{1+w_2}\right)} \times (1 + w_2 - aw_2)^{-3\left(\frac{-w_0w_2}{w_2(1+w_2)}\right)}, \quad (16)$$

$$E_{\text{PADEII}}^2 = \Omega_{r0}a^{-4} + \Omega_{m0}a^{-3} + (1 - [\Omega_{r0} + \Omega_{m0}]) \times a^{-3\left(\frac{w_1+w_2}{w_2}\right)} \times (1 + w_2 \ln a)^{3\left(\frac{w_1-w_0w_2}{w_2^2}\right)}, \quad (17)$$

where Ω_{m0} (density parameter), Ω_{r0} (radiation parameter) and $\Omega_{de0} = 1 - \Omega_{m0} - \Omega_{r0}$ (dark energy parameter). Moreover, following the above lines in the case of CPL parameterisation we have

$$\rho_{\text{de}}^{\text{CPL}} = \rho_{\text{de}}^{(0)} a^{-3(1+w_0+w_1)} \exp\{-3w_1(1-a)\} \quad (18)$$

and

$$E_{\text{CPL}}^2 = \Omega_{r0}a^{-4} + \Omega_{m0}a^{-3} + (1 - \Omega_{m0} - \Omega_{r0}) \times a^{-3(1+w_0+w_1)} \exp[-3w_1(1-a)], \quad (19)$$

Bellow, we study the performance of PADE cosmological parameterisation against the latest observational data. Specifically, we implement a statistical analy-

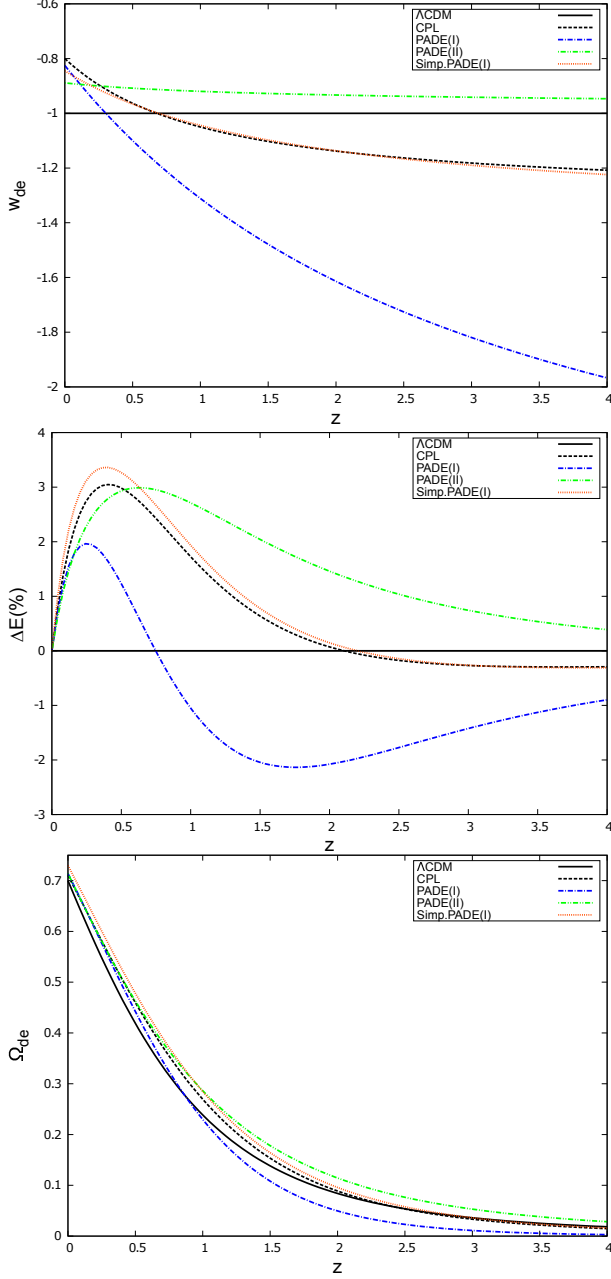


Figure 2. The redshift evolution of various cosmological quantities, namely dark energy EoS parameter $w_{de}(z)$ (top panel), relative deviation $\Delta E(\%) = [(E - E_\Lambda)/E_\Lambda] \times 100$ (middle panel) and $\Omega_{de}(z)$ (bottom panel). The different DE parameterisations are characterized by the colors and line-types presented in the inner panels of the figure.

sis using the background expansion data including those of SnIa (Suzuki et al. 2012), BAO (Beutler et al. 2011; Padmanabhan et al. 2012; Anderson et al. 2013; Blake et al. 2011a), CMB (Hinshaw et al. 2013), BBN (Serra et al. 2009; Burles et al. 2001), Hubble data (Moresco et al. 2012; Gaztanaga et al. 2009; Blake et al. 2012; Anderson et al. 2014). For more details concerning the expansion data, the $\chi^2(\mathbf{p})$ function, the Markov chain Monte Carlo (MCMC) analysis, the Akaike information criterion (AIC) and

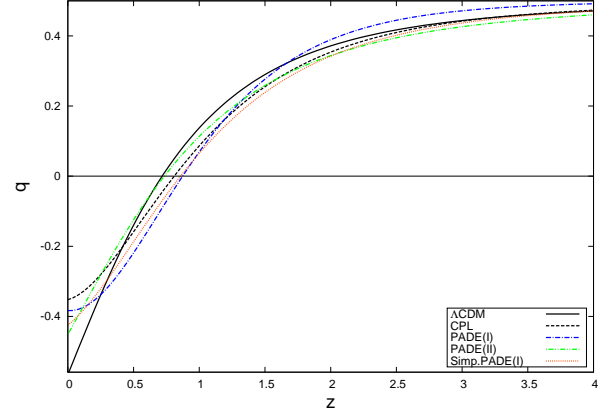


Figure 3. The evolution of the deceleration parameter q for different PADE parameterisations considered in this work. The CPL and Λ CDM models are shown for comparison.

the Bayesian information criterion (BIC) we refer the reader to Mehrabi et al. (2015b) (see also Basilakos et al. 2009b; Hinshaw et al. 2013; Mehrabi et al. 2015a, 2017; Malekjani et al. 2017). In this framework, the joint likelihood function is the product of the individual likelihoods:

$$\mathcal{L}_{\text{tot}}(\mathbf{p}) = \mathcal{L}_{\text{sn}} \times \mathcal{L}_{\text{bao}} \times \mathcal{L}_{\text{cmb}} \times \mathcal{L}_{\text{h}} \times \mathcal{L}_{\text{bbn}}, \quad (20)$$

which implies that the total chi-square χ_{tot}^2 is given by:

$$\chi_{\text{tot}}^2(\mathbf{p}) = \chi_{\text{sn}}^2 + \chi_{\text{bao}}^2 + \chi_{\text{cmb}}^2 + \chi_{\text{h}}^2 + \chi_{\text{bbn}}^2, \quad (21)$$

where the statistical vector \mathbf{p} includes the free parameters of the model. In our work the above vector becomes (a) $\mathbf{p} = \{\Omega_{\text{DM}0}, \Omega_{\text{b}0}, h, w_0, w_1, w_2\}$ for PADE (I) and (II) parameterisations, (b) $\mathbf{p} = \{\Omega_{\text{DM}0}, \Omega_{\text{b}0}, h, w_0, w_2\}$ for simplified PADE (I) and (c) $\mathbf{p} = \{\Omega_{\text{DM}0}, \Omega_{\text{b}0}, h, w_0, w_1\}$ in the case of CPL parameterisation. Notice that we utilize $\Omega_{\text{m}0} = \Omega_{\text{DM}0} + \Omega_{\text{b}0}$ and $h = H_0/100$, while the energy density of radiation is fixed to $\Omega_{\text{r}0} = 2.469 \times 10^{-5} h^{-2} (1.6903)$ (Hinshaw et al. 2013).

Additionally, we utilize the well know information criteria, namely AIC (Akaike 1974) and BIC (Schwarz 1978) in order to test the statistical performance of the cosmological models themselves. In particular, AIC and BIC are given by

$$\begin{aligned} \text{AIC} &= -2 \ln \mathcal{L}_{\text{max}} + 2k, \\ \text{BIC} &= -2 \ln \mathcal{L}_{\text{max}} + k \ln N, \end{aligned} \quad (22)$$

where k is the number of free parameters and N is the total number of observational data points. The results of our statistical analysis are presented in Tables (1) and (2) respectively. Although the current DE parameterisations provide low AIC values with respect to those of Λ CDM, we find $\Delta \text{AIC} = \text{AIC} - \text{AIC}_\Lambda < 4$ hence, the DE parameterisations explored in this study are consistent with the expansion data. In order to visualize the solution space of the model parameters in Fig.(1) we present the 1σ , 2σ and 3σ confidence levels for various parameter pairs. Using the best fit model parameters [see Table 2] in Fig. (2) we plot the redshift evo-

lution of w_{de} (upper panel), $\Delta E(\%) = [(E - E_\Lambda)/E_\Lambda] \times 100$ (middle panel) and Ω_{de} (lower panel). The different parameterisations are characterized by the colors and line-types presented in the caption of Fig. (2). We find that the EoS parameter of PADE II evolves only in the quintessence regime ($-1 < w_{\text{de}} < -1/3$). For the other DE parameterisations we observe that w_{de} varies in the phantom region ($w_{\text{de}} < -1$) at high redshifts, while it enters in the quintessence regime ($-1 < w_{\text{de}} < -1/3$) at relatively low redshifts. Notice, that the present value of w_{de} can be found in Table (2). From the middle panel of Fig. (2), we observe that the relative difference ΔE is close to 2 – 3.5% at low redshifts ($z \sim 0.5$), while in the case of PADE (II) we always have $E_{\text{PADEII}}(z) > E_\Lambda(z)$. Lastly, in the bottom panel of Fig.(2) we show the evolution of Ω_{de} , where its current value can be found in Table (2). As expected, Ω_{de} tends to zero at high redshifts since matter dominates the cosmic fluid. In the case of PADE parameterisations we observe that Ω_{de} is larger than that of the usual Λ cosmology.

Finally, we would like to estimate the transition redshift z_{tr} of the PADE parameterisations by utilizing the deceleration parameter $q(z) = -1 - \dot{H}/H^2$. Following, standard lines it is easy to show

$$\frac{\dot{H}}{H^2} = -\frac{3}{2} \left(1 + w_{\text{de}}(z) \Omega_{\text{de}}(z) \right) \quad (23)$$

which implies that

$$q(z) = \frac{1}{2} + \frac{3}{2} w_{\text{de}}(z) \Omega_{\text{de}}(z) \quad (24)$$

Using the best fit values of Table (2), we plot in Fig. (3) the evolution of q for the current DE parameterisations. In all cases, including that of Λ CDM, q tends to 1/2 at early enough times. This is expected since the universe is matter dominated ($\Omega_{\text{de}} \simeq 0$) at high redshifts. Now solving the $q(z_{\text{tr}}) = 0$ we can derive the transition redshift, namely the epoch at which the expansion of the universe starts to accelerate. In particular, we find $z_{\text{tr}} = 0.86$ (PADE I), $z_{\text{tr}} = 0.84$ (simplified PADE), $z_{\text{tr}} = 0.72$ (PADE II), $z_{\text{tr}} = 0.80$ (CPL) and $z_{\text{tr}} = 0.71$ (Λ CDM). The latter results are in good agreement with the measured z_{tr} based on the cosmic chronometer $H(z)$ data [Farooq et al. \(2017\)](#) (see also [Capozziello et al. 2014, 2015](#)).

4. GROWTH RATE IN DE PARAMETERISATIONS

In this section, we study the linear growth of matter perturbations in PADE cosmologies and we compare them with those of CPL and Λ CDM respectively. In this kind of studies the natural question to ask is the following: *how DE affects the linear growth of matter fluctuations?* In order to treat to answer this question we need to introduce the following two distinct situations, which have been considered within different approaches in the literature ([Armendariz-Picon et al. 1999](#); [Garriga & Mukhanov 1999](#); [Armendariz-Picon et al. 2000](#); [Erickson et al. 2002](#);

[Bean & Doré 2004](#); [Hu & Scranton 2004](#); [Abramo et al. 2007, 2008](#); [Ballesteros & Riotto 2008](#); [Abramo et al. 2009](#); [Basilakos et al. 2009a](#); [de Putter et al. 2010](#); [Pace et al. 2010](#); [Akhoury et al. 2011](#); [Sapone & Majerotto 2012](#); [Pace et al. 2012](#); [Batista & Pace 2013](#); [Dossett & Ishak 2013](#); [Batista 2014](#); [Basse et al. 2014](#); [Pace et al. 2014a,c,b](#); [Malekjani et al. 2015](#); [Naderi et al. 2015](#); [Mehrabi et al. 2015c,b,a](#); [Nazari-Pooya et al. 2016](#); [Malekjani et al. 2017](#)): (i) the scenario in which the DE component is homogeneous ($\delta_{\text{de}} \equiv 0$) and only the corresponding non-relativistic matter is allowed to cluster ($\delta_{\text{m}} \neq 0$) and (ii) the case in which the whole system clusters (both matter and DE). Owing to the fact that we are in the matter phase of the universe we can neglect the radiation term from the Hubble expansion.

4.1. Basic equations

The basic equations that govern the evolution of non-relativistic matter and DE perturbations are given by ([Abramo et al. 2009](#))

$$\dot{\delta}_{\text{m}} + \frac{\theta_{\text{m}}}{a} = 0, \quad (25)$$

$$\dot{\delta}_{\text{de}} + (1 + w_{\text{de}}) \frac{\theta_{\text{de}}}{a} + 3H(c_{\text{eff}}^2 - w_{\text{de}}) \delta_{\text{de}} = 0, \quad (26)$$

$$\dot{\theta}_{\text{m}} + H\theta_{\text{m}} - \frac{k^2 \phi}{a} = 0, \quad (27)$$

$$\dot{\theta}_{\text{de}} + H\theta_{\text{de}} - \frac{k^2 c_{\text{eff}}^2 \theta_{\text{de}}}{(1 + w_{\text{de}})a} - \frac{k^2 \phi}{a} = 0, \quad (28)$$

where k is the wave number and c_{eff} is the effective sound speed of perturbations ([Abramo et al. 2009](#); [Batista & Pace 2013](#); [Batista 2014](#)). Combining the Poisson equation

$$-\frac{k^2}{a^2} \phi = \frac{3}{2} H^2 [\Omega_{\text{m}} \delta_{\text{m}} + (1 + 3c_{\text{eff}}^2) \Omega_{\text{de}} \delta_{\text{de}}], \quad (29)$$

with Eqs. (27 & 28), eliminating θ_{m} and θ_{de} and changing the derivative from time to scale factor a , we obtain the following system of differential equations (see also [Mehrabi et al. 2015a](#); [Malekjani et al. 2017](#))

$$\delta_{\text{m}}'' + \frac{3}{2a} (1 - w_{\text{de}} \Omega_{\text{de}}) \delta_{\text{m}}' = \frac{3}{2a^2} [\Omega_{\text{m}} \delta_{\text{m}} + \Omega_{\text{de}} (1 + 3c_{\text{eff}}^2) \delta_{\text{de}}] \quad (30)$$

$$\delta_{\text{de}}'' + A \delta_{\text{de}}' + B \delta_{\text{de}} = \frac{3}{2a^2} (1 + w_{\text{de}}) [\Omega_{\text{m}} \delta_{\text{m}} + \Omega_{\text{de}} (1 + 3c_{\text{eff}}^2) \delta_{\text{de}}] \quad (31)$$

Bellow we set $c_{\text{eff}} \equiv 0$ which means that the whole system (matter and DE) fully clusters. Moreover, we remind reader that for homogeneous DE models we have $\delta_{\text{de}} \equiv 0$, hence Eq.(30) reduces to the well known differential equation of [Peebles \(1993\)](#) [see also [Pace et al. \(2010\)](#) and references therein]. Concerning the functional forms of A and B we have

$$A = \frac{1}{a} \left[-3w_{\text{de}} - \frac{aw'_{\text{de}}}{1 + w_{\text{de}}} + \frac{3}{2} (1 - w_{\text{de}} \Omega_{\text{de}}) \right],$$

$$B = \frac{1}{a^2} \left[-aw'_{\text{de}} + \frac{aw'_{\text{de}} w_{\text{de}}}{1 + w_{\text{de}}} - \frac{1}{2} w_{\text{de}} (1 - 3w_{\text{de}} \Omega_{\text{de}}) \right] \quad (32)$$

Table 2. A summary of the best-fit parameters for the various DE parameterisations using the background data.

Model	PADE I	simplified PADE I	PADE II	CPL	Λ CDM
$\Omega_m^{(0)}$	0.286 ± 0.010	0.270 ± 0.010	0.2864 ± 0.0096	0.2896 ± 0.0090	0.2891 ± 0.0090
h	0.682 ± 0.012	0.682 ± 0.012	0.686 ± 0.013	0.682 ± 0.012	0.6837 ± 0.0084
w_0	-0.825 ± 0.091	-0.845 ± 0.039	-0.889 ± 0.080	-0.80 ± 0.11	—
w_1	$-0.09^{+0.39}_{-0.32}$	—	$0.37^{+0.29}_{-0.23}$	$-0.51^{+0.48}_{-0.38}$	—
w_2	$-0.683^{+0.040}_{-0.034}$	-0.387 ± 0.034	$-0.353^{+0.038}_{-0.034}$	—	—
$w_{de}(z=0)$	-0.825	-0.845	-0.889	-0.80	-1.0
$\Omega_{de}(z=0)$	0.714	0.730	0.7136	0.7104	0.7109

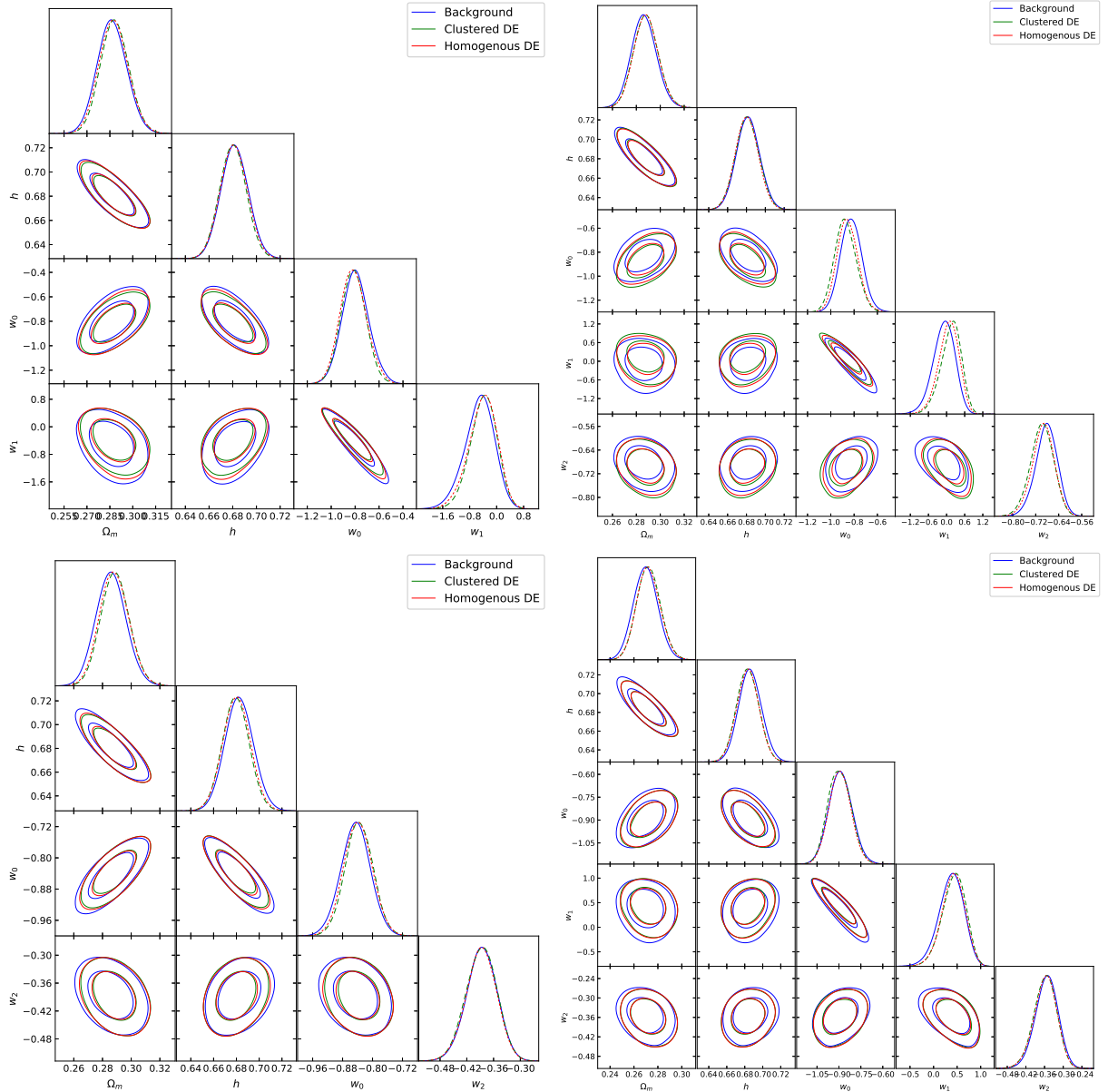
**Figure 4.** The 1σ and 2σ likelihood contours for various planes using the solely expansion data (blue), combined expansion and growth rate data for clustered (green) and homogeneous (red) DE parameterisations. The upper left (upper right) shows the results for CPL (PADE I) parameterisation. The lower left (lower right) shows the results for simplified PADE I (PADE II) parameterisation.

Table 3. The statistical results for homogeneous (clustered) DE parameterisations used in the analysis. These results are based on the expansion+growth rate data. The concordance Λ CDM model is shown for comparison.

Model	PADE I	simplified PADE I	PADE II	CPL	Λ CDM
k	7	6	7	6	4
χ^2_{\min}	576.4(576.5)	576.4(576.7)	576.9(577.1)	576.5(576.7)	582.6
AIC	590.4(590.5)	588.4(588.7)	590.9(591.1)	588.5(588.7)	590.6
BIC	621.6(621.7)	615.1(615.4)	622.1(622.3)	615.2(615.4)	608.4

Table 4. A summary of the best-fit parameters for homogeneous (clustered) DE parameterisations using the background+growth rate data.

Model	PADE I	simplified PADE I	PADE II	CPL	Λ CDM
$\Omega_m^{(0)}$	0.288 ± 0.010 (0.288 \pm 0.010)	0.288 ± 0.010 (0.2888 \pm 0.0099)	0.2721 ± 0.0097 (0.2723 \pm 0.0098)	0.2875 ± 0.0095 (0.2882 \pm 0.0093)	0.2902 ± 0.0090
h	0.681 ± 0.012 (0.681 \pm 0.012)	0.680 ± 0.012 (0.679 \pm 0.012)	0.684 ± 0.012 (0.683 \pm 0.012)	0.681 ± 0.011 (0.680 \pm 0.011)	0.6833 ± 0.0084
w_0	-0.856 ± 0.088 ($-0.874^{+0.086}_{-0.097}$)	-0.839 ± 0.038 (-0.836 ± 0.037)	-0.893 ± 0.075 (-0.896 ± 0.078)	$-0.81^{+0.10}_{-0.12}$ (-0.81 ± 0.10)	–
w_1	$0.07^{+0.37}_{-0.29}$ ($0.14^{+0.38}_{-0.29}$)	–	$0.41^{+0.26}_{-0.22}$ ($0.43^{+0.27}_{-0.22}$)	$-0.41^{+0.46}_{-0.37}$ ($-0.39^{+0.42}_{-0.36}$)	–
w_2	$-0.694^{+0.040}_{-0.036}$ ($-0.699^{+0.042}_{-0.038}$)	-0.388 ± 0.034 (-0.388 ± 0.035)	$-0.357^{+0.039}_{-0.033}$ ($-0.358^{+0.038}_{-0.034}$)	–	–
σ_8	0.751 ± 0.015 (0.755 \pm 0.016)	0.751 ± 0.015 (0.758 \pm 0.015)	0.771 ± 0.015 (0.771 \pm 0.016)	0.751 ± 0.015 (0.756 \pm 0.015)	0.744 ± 0.014
$w_{de}(z=0)$	-0.856 (-0.874)	-0.839 (-0.836)	-0.893 (-0.896)	-0.81 (-0.81)	-1.0
$\Omega_{de}(z=0)$	0.712 (0.712)	0.712 (0.7112)	0.7279 (0.7277)	0.7125 (0.7118)	0.7098

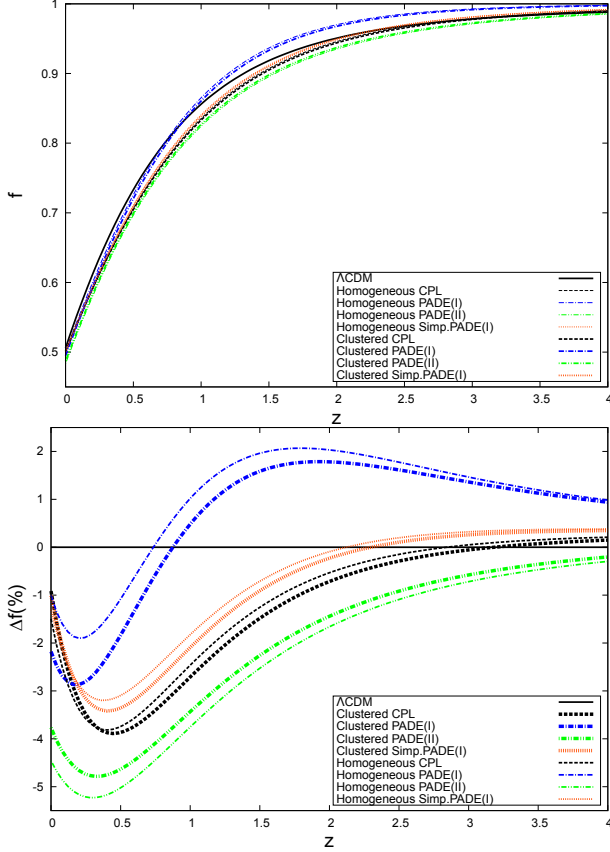


Figure 5. The redshift evolution of the growth rate function $f(z)$ (top-panel) and the corresponding fractional difference $\Delta f(\%) = 100 \times [f(z) - f_{\Lambda}(z)]/f_{\Lambda}(z)$ (bottom panel). The different DE parameterisations are characterized by the colors and line-types presented in the inner panels of the figure

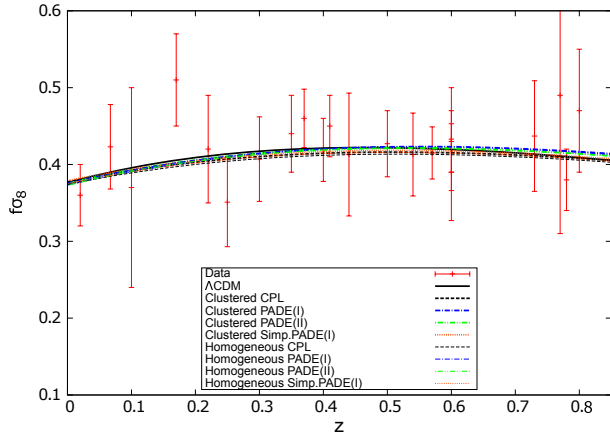


Figure 6. Comparison of the observed and theoretical evolution of the growth rate $f(z)\sigma_8(z)$ as a function of redshift z . Open squares correspond to the data. Line-types and colors are explained in the inner plot of the figure.

In order to perform the numerical integration of the above system (30 & 31) it is crucial to introduce the appropriate initial conditions. Here we utilize (see also [Batista & Pace](#)

[2013](#); [Mehrabi et al. 2015a](#); [Malekjani et al. 2017](#))

$$\begin{aligned} \delta'_{mi} &= \frac{\delta_{mi}}{a_i}, \\ \delta_{dei} &= \frac{1 + w_{dei}}{1 - 3w_{dei}} \delta_{mi}, \\ \delta'_{dei} &= \frac{4w'_{dei}}{(1 - 3w_{dei})^2} \delta_{mi} + \frac{1 + w_{dei}}{1 - 3w_{dei}} \delta'_{mi}, \end{aligned} \quad (33)$$

where we fix $a_i = 10^{-4}$ and $\delta_{mi} = 1.5 \times 10^{-5}$. In fact using the aforementioned conditions we verify that matter perturbations always stay in the linear regime. From the technical viewpoint, using w_{de} , Ω_{de} we can solve the system of equations (30 & 31) which means that the fluctuations (δ_{de}, δ_m) can be readily calculated, and from them $f(z) = d \ln \delta_m / d \ln a$, $\sigma_8(z) = \frac{\delta_m(z)}{\delta_m(z=0)} \sigma_8(z=0)$ (rms mass variance at $R = 8h^{-1} Mpc$) and $f(z)\sigma_8(z)$ immediately ensue.

Now we perform a joint statistical analysis involving the expansion data (see Sect. 3) and the growth data. In principle, this can help us to understand better the theoretical expectations of the present DE parameterisations, as well as to test their behaviour at the background and at the perturbation level. The growth data and the details regarding the likelihood analysis (χ^2_{gr} , MCMC algorithm etc) can be found in Sect. 3 of our previous work ([Mehrabi et al. 2015a](#)). Briefly, in order to obtain the overall likelihood function we need to include the likelihood function of the growth data in Eq.(20) as follows

$$\mathcal{L}_{tot}(\mathbf{p}) = \mathcal{L}_{sn} \times \mathcal{L}_{bao} \times \mathcal{L}_{cmb} \times \mathcal{L}_h \times \mathcal{L}_{bbn} \times \mathcal{L}_{gr}, \quad (34)$$

hence

$$\chi^2_{tot}(\mathbf{p}) = \chi^2_{sn} + \chi^2_{bao} + \chi^2_{cmb} + \chi^2_h + \chi^2_{bbn} + \chi^2_{gr}, \quad (35)$$

where the statistical vector \mathbf{p} contains an additional free parameter, namely $\sigma_8 \equiv \sigma_8(z=0)$.

In Tables (3) and (4) we show the resulting best fit values for various DE parameterisations under study, in which we also provide the observational constraints of the clustered DE parameterisations. Furthermore, in Fig. (4) we present the 1σ and 2σ contours for various parameter pairs. The blue contour represents the confidence levels based on geometrical data and green (red) contours show the confidence levels based on geometrical + growth rate data for clustered (homogeneous) DE parameterisations. Comparing the latter results with those of see Sect. 3 we conclude that the observational constraints which are placed by the expansion+growth data are practically the same with those found by the expansion data. Therefore, we can use the current growth data in order to put constrains only on σ_8 , since they do not significantly affect the rest of the cosmological parameters. This means that the results of see Sect. 3 concerning evolution of the main cosmological functions (w_{de} , $E(z)$ and Ω_{de}) remain unaltered. To this end, in Fig. (5) we plot the evolution of growth rate $f(z)$ as a function of redshift (upper panel)

and the fractional difference with respect to that of Λ CDM model (lower panel), $\Delta f(\%) = 100 \times [f(z) - f_\Lambda(z)]/f_\Lambda(z)$. Specifically, in the range of $0 \leq z \leq 4$ we find:

- for homogeneous (or clustered) PADE I parameterisation the relative difference is $\sim [-1\%, 1\%]$ (or $\sim [-2.25\%, 1\%]$)
- in the case of simplified PADE I we have $\sim [-1\%, 0.4\%]$ and $\sim [-1\%, 0.4\%]$ for homogeneous and clustered DE respectively
- for homogeneous (or clustered) PADE II DE the relative deviation lies in the interval $\sim [-4.25\%, -0.25\%]$ (or $\sim [-4\%, -0.25\%]$). Finally, in the case of CPL parameterisation we obtain $\sim [-1.5\%, 0.1\%]$ (homogeneous) and $\sim [-1\%, 0.1\%]$ (clustered).

In this context, we verify that at high redshifts the growth rate tends to unity since the universe is matter dominated, namely $\delta_m \propto a$. Moreover, we observe that the evolution of Δf has one maximum/minimum and one zero point. As expected, this feature of Δf is related to the evolution of ΔE (see middle panel of Fig. 2). Indeed, we verify that large values of the normalized Hubble parameter $E(z)$ correspond to small values of the growth rate. Also, looking at Fig. 2 (middle panel) and Fig. 5 (bottom panel) we easily see that when ΔE has a maximum the growth rate Δf has a minimum and vice versa. We also observe that if $\Delta E < 0$ then $\Delta f > 0$ and vice versa. Finally, in Fig. (6), we compare the observed $f\sigma_8(z)$ with the predicted growth rate function of the current DE parameterisations [for curves see caption of Fig. (6)]. We find that all parameterisations represent well the growth data. As expected from AIC and BIC analysis (see Table 3) the current DE parameterisations and standard Λ CDM cosmology are all consistent with current observational data.

4.2. The growth index

We would like to finish this section with a discussion concerning the growth index of matter fluctuations γ , which affects the growth rate of clustering via the following relation (first introduced by Peebles 1993)

$$f(z) = \frac{d \ln \delta_m}{d \ln a}(z) \simeq \Omega_m^\gamma(z). \quad (36)$$

The theoretical formula of the growth index has been studied for various cosmological models, including scalar field DE (Silveira & Waga 1994; Wang & Steinhardt 1998b; Linder & Jenkins 2003; Lue et al. 2004; Linder & Cahn 2007; Nesseris & Perivolaropoulos 2008), DGP (Linder & Cahn 2007; Gong 2008; Wei 2008; Fu et al. 2009), Finsler-Randers (Basilakos & Stavrinos 2013), running vacuum $\Lambda(H)$ (Basilakos & Sola 2015), $f(R)$ (Gannouji et al. 2009; Tsujikawa et al. 2009), $f(T)$ (Basilakos 2016), Holographic DE (Mehrabi et al. 2015a)

and Agegraphic DE (Malekjani et al. 2017) If we combine equations (25-28), (29) and using simultaneously $\frac{d\delta_m}{dt} = aH \frac{d\delta_m}{da}$ then we obtain (see also Abramo et al. 2007, 2009; Mehrabi et al. 2015a)

$$a^2 \delta_m'' + a \left(3 + \frac{\dot{H}}{H^2} \right) \delta_m' = \frac{3}{2} \Omega_m \mu, \quad (37)$$

where

$$\frac{\dot{H}}{H^2} = \frac{d \ln H}{d \ln a} = -\frac{3}{2} - \frac{3}{2} w_{de}(a) \Omega_{de}(a), \quad (38)$$

and $\Omega_{de}(a) = 1 - \Omega_m(a)$. The quantity $\mu(a)$ characterizes the nature of DE in PADE parametrisations, namely

$$\mu(a) = \begin{cases} 1 & \text{Homogeneous PADE} \\ 1 + \frac{\Omega_{de}(a)}{\Omega_m(a)} \Delta_{de}(a) (1 + 3c_{eff}^2) & \text{Clustered PADE} \end{cases} \quad (39)$$

where we have set $\Delta_{de} \equiv \delta_{de}/\delta_m$. Obviously, if we use $c_{eff}^2 = 0$ then Eq.(37) reduces to Eq.(30), while in the case of the usual Λ CDM model we need to a priori set $\delta_{de} \equiv 0$.

Furthermore, substituting Eq.(36) and Eq.(38) in Eq.(37) we arrive at

$$-(1+z) \frac{d\gamma}{dz} \ln(\Omega_m) + \Omega_m^\gamma + 3w_{de} \Omega_{de} \left(\gamma - \frac{1}{2} \right) + \frac{1}{2} = \frac{3}{2} \Omega_m^{1-\gamma} \mu. \quad (40)$$

Regarding the growth index evolution we use the following phenomenological parameterisation (see also Polarski & Gannouji 2008; Wu et al. 2009; Bueno Belloso et al. 2011; Di Porto et al. 2012; Ishak & Dossett 2009; Basilakos 2012; Basilakos & Pouri 2012)

$$\gamma(a) = \gamma_0 + \gamma_1 [1 - a(z)]. \quad (41)$$

Now, utilizing Eq.(40) at the present time $z = 0$ and with the aid of Eq.(41) we obtain (see also Polarski & Gannouji 2008)

$$\gamma_1 = \frac{\Omega_{m0}^{\gamma_0} + 3w_{de0}(\gamma_0 - \frac{1}{2})\Omega_{de0} + \frac{1}{2} - \frac{3}{2}\Omega_{m0}^{1-\gamma_0}\mu_0}{\ln \Omega_{m0}}, \quad (42)$$

where $\mu_0 = \mu(z = 0)$ and $w_{de0} = w_{de}(z = 0)$. Clearly, in order to predict the growth index evolution in DE models we need to estimate the value of γ_0 . For the current parameterisation it is easy to show that at high redshifts $z \gg 1$ the asymptotic value of $\gamma(z)$ is written as $\gamma_\infty \simeq \gamma_0 + \gamma_1$, while the theoretical formula of γ_∞ is given by Steigerwald et al. (2014)

$$\gamma_\infty = \frac{3(M_0 + M_1) - 2(H_1 + N_1)}{2 + 2X_1 + 3M_0} \quad (43)$$

where the following quantities have been defined:

$$M_0 = \mu|_{\omega=0}, \quad M_1 = \left. \frac{d\mu}{d\omega} \right|_{\omega=0} \quad (44)$$

and

$$N_1 = 0, \quad H_1 = -\frac{X_1}{2} = \frac{3}{2} w_{de}(a)|_{\omega=0}, \quad (45)$$

where $\omega = \ln \Omega_m(a)$. Obviously, for $z \gg 1$ we get $\Omega_m(a) \rightarrow 1$ [or $\Omega_{de}(a) \rightarrow 0$] which implies $\omega \rightarrow 0$. For more details regarding the theoretical treatment of (43) we refer the reader to Steigerwald et al. (2014). It is interesting to mention that the asymptotic value of the equation of state parameter for the current PADE cosmologies is written as

$$w_\infty \equiv w_{de}(a \rightarrow 0) = \begin{cases} \frac{w_0 + w_1}{1 + w_2}, & \text{for PADE I} \\ \frac{w_0}{1 + w_1}, & \text{for Sim. PADE I} \\ \frac{w_1}{w_2}, & \text{for PADE II.} \end{cases} \quad (46)$$

At this point we are ready to present our growth index results:

- **Homogeneous PADE parameterisations:** here we set $\mu(a) = 1$ ($\Delta_{de} \equiv 0$). From Eqs.(44) and (45) we find

$$\{M_0, M_1, H_1, X_1\} = \left\{1, 0, \frac{3w_\infty}{2}, -3w_\infty\right\}$$

and thus Eq.(43) becomes

$$\gamma_\infty = \frac{3(w_\infty - 1)}{6w_\infty - 5}. \quad (47)$$

Lastly, inserting $\gamma_0 \simeq \gamma_\infty - \gamma_1$ into Eq.(42) and utilizing Eqs. (46-47) together with the cosmological constraints of Table (4) we obtain

$$(\gamma_0, \gamma_1, \gamma_\infty) = \begin{cases} (0.555, -0.031, 0.524), & \text{for PADE I} \\ (0.558, -0.021, 0.537), & \text{for Sim. PADE I} \\ (0.559, -0.017, 0.542), & \text{for PADE II.} \end{cases} \quad (48)$$

For comparison we provide the results for the Λ CDM model and CPL parameterisation respectively. Specifically, we find $(\gamma_0, \gamma_1, \gamma_\infty)_\Lambda \simeq (0.556, -0.011, 0.545)$ and $(\gamma_0, \gamma_1, \gamma_\infty)_{\text{CPL}} \simeq (0.561, -0.020, 0.541)$.

- **Clustered PADE parameterisations:** here the functional form of $\mu(a)$ is given by the second branch of Eq.(39) which means that we need to define Δ_{de} . From Eq.(33) we simply have $\Delta_{de} = \frac{1 + w_{de}}{1 - 3w_{de}}$ and thus $\mu(a)$ takes the following form

$$\mu(a) = 1 + (1 + 3c_{\text{eff}}^2) \frac{\Omega_{de}}{\Omega_m} \frac{(1 + w_{de})}{(1 - 3w_{de})}. \quad (49)$$

In this case, from Eqs.(44) and (45) we obtain (for more details see the Appendix)

$$\{M_0, M_1, H_1, X_1\} = \left\{1, -\frac{(1 + w_\infty)(1 + 3c_{\text{eff}}^2)}{1 - 3w_\infty}, \frac{3w_\infty}{2}, -3w_\infty\right\}$$

and from Eq.(43) we find

$$\gamma_\infty \simeq \frac{3[(1 - 3w_\infty)(1 - w_\infty) - (1 + w_\infty)(1 + c_{\text{eff}}^2)]}{(6w_\infty - 5)(3w_\infty - 1)}.$$

Notice, that in the case of fully clustered PADE parameterisations ($c_{\text{eff}}^2 = 0$) the above expression becomes

$$\gamma_\infty \simeq \frac{3w_\infty(3w_\infty - 5)}{(6w_\infty - 5)(3w_\infty - 1)}. \quad (50)$$

(46-47) Now, utilizing Eqs.(46-50) and the cosmological parameters of Table (4) we find

$$(\gamma_0, \gamma_1, \gamma_\infty) = \begin{cases} (0.547, 0.005, 0.552), & \text{for PADE I} \\ (0.542, 0.012, 0.554), & \text{for Sim. PADE I} \\ (0.549, 0.003, 0.552), & \text{for PADE II.} \end{cases} \quad (51)$$

To this end, if the CPL parameterisation is allowed to cluster then the asymptotic value of the growth index is given by Eq.(50), where $w_\infty = w_0 + w_1$. In this case we find $(\gamma_0, \gamma_1, \gamma_\infty)_{\text{CPL}} \simeq (0.539, 0.013, 0.552)$.

In Table (5), we provide a compact presentation of our numerical results including the relative fractional difference $\Delta\gamma(\%) = [(\gamma - \gamma_\Lambda)/\gamma_\Lambda] \times 100$ between all DE parameterisations and the concordance Λ cosmology, in 3 distinct redshift bins. Overall, we find that the fractional deviation lies in the interval $\sim [-2.2\%, 0.3\%]$. We believe that relative differences of $|\Delta\gamma| \leq 1\%$ will be difficult to detect even with the next generation of surveys, based mainly on Euclid (see Taddei & Amendola 2015). Using the latter forecast and the results presented in section 4, we can now divide the current DE parameterisations into those that can be distinguished observationally and those that are practically indistinguishable from Λ CDM model. The former DE parameterisations are the following three: homogeneous PADE I, clustered Simplified PADE I and clustered CPL. However, the reader has to remember that these results are based on utilizing cosmological parameters that have been fitted by the present day observational data (see Table 4). Therefore, if future observational data would provide slightly different values for the parameters of DE parameterisations then the growth rate predictions of the studied DE parameterisations could be somewhat different than those derived here.

5. CONCLUSIONS

We studied the cosmological properties of various DE parameterisations in which the EoS parameter is given with the aid of the PADE approximation. Specifically, using different types of PADE parameterisation we investigated the behaviour of various DE scenarios at the background and at the perturbation levels.

Table 5. Numerical results. The 1st and the 2nd columns indicate the status of DE and the corresponding parametrisation. 3rd, 4th and 5th columns show the γ_0 , γ_1 and $\Delta_{\text{de}0}$ values. The remaining columns present the fractional relative difference between the DE parameterisations and the Λ CDM cosmology based on the cosmological parameters appeared in Table 4.

DE Status	DE Parametrisation	γ_0	γ_1	$\Delta_{\text{de}0}$	$\Delta\gamma(\%)$		
					$z < 0.5$	$0.5 \leq z < 1$	$1 \leq z < 1.5$
Homogeneous	PADE I	0.555	-0.031		-1.2	-1.8	-2.2
	Sim. PADE I	0.558	-0.021		-0.1	-0.4	-0.6
	PADE II	0.559	-0.017		0.15	-0.01	-0.15
	CPL	0.561	-0.02		0.3	-0.02	-0.2
Clustered	PADE I	0.547	0.005	0.035	-0.8	-0.5	-0.1
	Sim. PADE I	0.542	0.012	0.047	-1.4	-0.7	-0.2
	PADE II	0.549	0.003	0.028	-0.6	-0.4	-0.02
	CPL	0.539	0.013	0.055	-2	-1.5	-0.8

The main results of the present study are summarized as follows:

(i) Initially, using the latest expansion data we performed a likelihood analysis in the context of Markov Chain Monte Carlo (MCMC) method. It is interesting to mention that the statistical performance of the MCMC method has been discussed in Capozziello et al. (2011) and references therein. Specifically, these authors showed that if we have a multi-dimensional space of the cosmological parameters then the MCMC algorithm provides better constraints than other popular fitting procedures. The results of our analysis for the explored PADE cosmologies, including those of CPL and Λ CDM can be found in Tables (1 & 2). Based on this analysis we placed constraints on the model parameters and we found that all DE parameterisations are consistent with the expansion data. In this framework, using the best fit values we found that only the PADE (II) parameterisation remains in the quintessence regime ($1 < w_{\text{de}} < 1/3$). The rest of the PADE parameterisations evolves in the phantom region ($w_{\text{de}} < -1$) at high redshifts, while they enter in the quintessence regime at relatively low redshifts. Concerning the cosmic expansion we found that prior to the present time the Hubble parameter of the DE parameterisations (PADE and CPL) is $\sim 2 - 3.5\%$ larger than the Λ CDM cosmological model. We also showed that the transition redshift from decelerating to accelerating expansion in the context of PADE parameterisations is consistent with that (Farooq et al. 2017) using the cosmic chronometer $H(z)$ data. Notice, that similar results found in the framework of modified theory of gravities (Capozziello et al. 2014, 2015).

(ii) Then, we studied for the first time the growth of perturbations in homogeneous and clustered PADE cosmologies. First we used a joint statistical analysis involving the expansion data and the growth data in order to place constraints on σ_8 . Second, based on the best fit cosmological

parameters we computed the evolution of the growth rate of clustering $f(z)$. For the current DE parameterisations we found that the growth rate function is lower than Λ CDM model at low redshifts, while the differences among the parameterisations are negligible at high redshifts. Third, following the notations of Steigerwald et al. (2014) we derived the functional form of the growth index (γ) of linear matter perturbations. Assuming that DE is homogeneous we found the well known asymptotic value of the growth index, namely $\gamma_\infty = \frac{3(w_\infty - 1)}{6w_\infty - 5}$ [$w_\infty = w(z \rightarrow \infty)$], while in the case of clustered DE parameterisations we obtained $\gamma_\infty \simeq \frac{3w_\infty(3w_\infty - 5)}{(6w_\infty - 5)(3w_\infty - 1)}$.

Finally, utilizing the fractional deviation between all DE parameterisations and the concordance Λ cosmology we found that $\Delta\gamma \sim [-2.2\%, 0.3\%]$. We concluded that relative differences of $|\Delta\gamma| \leq 1\%$ will be difficult to detect even with the next generation of surveys, based on Euclid (see Taddei & Amendola 2015). Combining the latter forecast and the results presented in section 4, we divided the current DE parameterisations into those that can be distinguished observationally and those that are practically indistinguishable from Λ CDM. The former DE parameterisations are the following three: homogeneous PADE I, clustered Simplified PADE I and clustered CPL.

6. ACKNOWLEDGEMENTS

MM and AM acknowledge support from the Iran Science Elites Federation. DFM acknowledges support from the Research Council of Norway, and the NOTUR facilities. SB acknowledges support by the Research Center for Astronomy of the Academy of Athens in the context of the program "Testing general relativity on cosmological scales" (ref. number 200/872).

APPENDIX

A. M_1 COEFFICIENT FOR CLUSTERED DARK ENERGY MODELS

Here we provide some details concerning the coefficient M_1 which appears in Eq.(43). This coefficient is given in terms of the variable $\omega = \ln\Omega_m$ (see section 4.1) which means that when $a \rightarrow 0$ ($z \gg 1$) we get $\Omega_m \rightarrow 1$ (or $\omega \rightarrow 0$). From Eq.(44) we have

$$M_1 = \left. \frac{d\mu}{d\omega} \right|_{\omega=0} = \Omega_m \left. \frac{d\mu}{d\Omega_m} \right|_{\Omega_m=1}.$$

Of course, in the case of homogeneous dark energy, namely $\mu(a) = 1$ we simply find $M_1 = 0$. However, if dark energy is allowed to cluster then the situation becomes quite different.

Indeed, using Eq.(49) we obtain after some calculations

$$\begin{aligned} \frac{d\mu}{d\Omega_m} &= (1 + 3c_{\text{eff}}^2) \frac{d}{d\Omega_m} \left(\frac{\Omega_{\text{de}}}{\Omega_m} \right) \frac{1 + w_{\text{de}}}{1 - 3w_{\text{de}}} + (1 + 3c_{\text{eff}}^2) \\ &\quad \times \frac{\Omega_{\text{de}}}{\Omega_m} \frac{d}{d\Omega_m} \left(\frac{1 + w_{\text{de}}}{1 - 3w_{\text{de}}} \right) \end{aligned}$$

where $\Omega_{\text{de}} = 1 - \Omega_m$,

$$\begin{aligned} \frac{d}{d\Omega_m} \left(\frac{\Omega_{\text{de}}}{\Omega_m} \right) &= -\frac{1}{\Omega_m^2}, \\ \frac{d}{d\Omega_m} \left(\frac{1 + w_{\text{de}}}{1 - 3w_{\text{de}}} \right) &= \frac{d}{da} \left(\frac{1 + w_{\text{de}}}{1 - 3w_{\text{de}}} \right) \frac{da}{d\Omega_m} \end{aligned}$$

with

$$\frac{d\Omega_m}{da} = \frac{3}{a} \Omega_m (1 - \Omega_m) w_{\text{de}} = \frac{3}{a} \Omega_m \Omega_{\text{de}} w_{\text{de}}.$$

Obviously, based on the above equations we arrive at

$$\begin{aligned} \Omega_m \frac{d\mu}{d\Omega_m} &= -(1 + 3c_{\text{eff}}^2) \frac{1 + w_{\text{de}}}{\Omega_m (1 - 3w_{\text{de}})} + (1 + 3c_{\text{eff}}^2) \frac{a}{3\Omega_m w_{\text{de}}} \\ &\quad \times \frac{d}{da} \left(\frac{1 + w_{\text{de}}}{1 - 3w_{\text{de}}} \right) \end{aligned}$$

Taking the limit $\Omega_m \rightarrow 1$ ($a \rightarrow 0$) of the latter expression we calculate M_1

$$M_1 = \Omega_m \left. \frac{d\mu}{d\Omega_m} \right|_{\Omega_m=1} = -(1 + 3c_{\text{eff}}^2) \frac{1 + w_{\text{de}}}{1 - 3w_{\text{de}}}.$$

REFERENCES

- Abramo, L. R., Batista, R. C., Liberato, L., & Rosenfeld, R. 2007, JCAP, 11, 12
— 2008, Phys. Rev. D, 77, 067301
— 2009, Phys. Rev., D79, 023516
Adachi, M., & Kasai, M. 2012, Prog. Theor. Phys., 127, 145
Akaike, H. 1974, IEEE Transactions of Automatic Control, 19, 716
Akhoury, R., Garfinkle, D., & Saotome, R. 2011, JHEP, 04, 096
Alcaniz, J. S. 2004, Phys. Rev., D69, 083521
Allen, S. W., Schmidt, R. W., Ebeling, H., Fabian, A. C., & van Speybroeck, L. 2004, Mon. Not. Roy. Astron. Soc., 353, 457
Amendola, L., Kunz, M., & Sapone, D. 2008, JCAP, 0804, 013
Amendola, L., et al. 2013, Living Rev. Rel., 16, 6
Anderson, L., Aubourg, E., Bailey, S., et al. 2013, MNRAS, 427, 3435
Anderson, L., et al. 2014, Mon. Not. Roy. Astron. Soc., 441, 24
Armendariz-Picon, C., Damour, T., & Mukhanov, V. F. 1999, Phys. Lett., B458, 209
Armendariz-Picon, C., Mukhanov, V., & Steinhardt, P. J. 2001, Phys. Rev. D, 63(10), 103510
Armendariz-Picon, C., Mukhanov, V. F., & Steinhardt, P. J. 2000, Phys. Rev. Lett., 85, 4438
Aviles, A., Bravetti, A., Capozziello, S., & Luongo, O. 2014, Phys. Rev., D90, 043531
Baker, A., & Graves-Morris, P. 1996, Pade Approximants (Cambridge University Press)
Ballesteros, G., & Riotto, A. 2008, Phys. Lett. B, 668, 171
Barboza, E. M., Alcaniz, J. S., Zhu, Z. H., & Silva, R. 2009, Phys. Rev., D80, 043521
Basilakos, S. 2012, International Journal of Modern Physics D, 21, 50064
Basilakos, S. 2015, Mon. Not. Roy. Astron. Soc., 449, 2151
— 2016, Phys. Rev., D93, 083007
Basilakos, S., Bueno Sanchez, J., & Perivolaropoulos, L. 2009a, Phys. Rev. D, 80, 043530
Basilakos, S., Plionis, M., & Lima, J. A. S. 2010, Phys. Rev., D82, 083517
Basilakos, S., Plionis, M., & Sola, J. 2009b, Phys. Rev., D80, 083511
Basilakos, S., & Pouri, A. 2012, MNRAS, 423, 3761
Basilakos, S., & Sola, J. 2015, Phys. Rev., D92, 123501
Basilakos, S., & Stavrinos, P. 2013, Phys. Rev., D87, 043506

- Basilakos, S., & Voglis, N. 2007, *Mon. Not. Roy. Astron. Soc.*, 374, 269
- Basse, T., Bjaelde, O. E., Hamann, J., Hannestad, S., & Wong, Y. Y. 2014, *JCAP*, 1405, 021
- Bassett, B. A., Brownstone, M., Cardoso, A., et al. 2008, *JCAP*, 0807, 007
- Batista, R., & Pace, F. 2013, *JCAP*, 1306, 044
- Batista, R. C. 2014, *Phys. Rev. D*, 89, 123508
- Bean, R., & Doré, O. 2004, *Phys. Rev. D*, 69, 083503
- Benjamin, J., Heymans, C., Semboloni, E., et al. 2007, *Mon. Not. Roy. Astron. Soc.*, 381, 702
- Beutler, F., Blake, C., Colless, M., et al. 2011, *MNRAS*, 416, 3017
- Blake, C., Kazin, E., Beutler, F., et al. 2011a, *MNRAS*, 418, 1707
- Blake, C., et al. 2011b, *Mon. Not. Roy. Astron. Soc.*, 415, 2876
- . 2012, *Mon. Not. Roy. Astron. Soc.*, 425, 405
- Bonilla Rivera, A., & Farieta, J. G. 2016, arXiv:1605.01984
- Bueno Belloso, A., García-Bellido, J., & Sapone, D. 2011, *JCAP*, 10, 10
- Burles, S., Nollett, K. M., & Turner, M. S. 2001, *ApJ*, 552, L1
- Caldwell, R. R. 2002, *Phys. Lett. B*, 545, 23
- Caldwell, R. R., Dave, R., & Steinhardt, P. J. 1998, *Phys. Rev. Lett.*, 80, 1582
- Capozziello, S., Farooq, O., Luongo, O., & Ratra, B. 2014, *Phys. Rev.*, D90, 044016
- Capozziello, S., Lazkoz, R., & Salzano, V. 2011, *Phys. Rev.*, D84, 124061
- Capozziello, S., Luongo, O., & Saridakis, E. N. 2015, *Phys. Rev.*, D91, 124037
- Carroll, S. M. 2001, *Living Reviews in Relativity*, 380, 1
- Chevallier, M., & Polarski, D. 2001, *IJMP D*, 10, 213
- Chuang, C.-H., et al. 2013, *Mon. Not. Roy. Astron. Soc.*, 433, 3559
- Cole, S., et al. 2005, *MNRAS*, 362, 505
- Contreras, C., et al. 2013, arXiv:1302.5178, [*Mon. Not. Roy. Astron. Soc.*430,924(2013)]
- Cooray, A., Huterer, D., & Baumann, D. 2004, *Phys. Rev.*, D69, 027301
- Copeland, E. J., Sami, M., & Tsujikawa, S. 2006, *IJMP D*, 15, 1753
- Corasaniti, P.-S., Giannantonio, T., & Melchiorri, A. 2005, *Phys. Rev.*, D71, 123521
- de Putter, R., Huterer, D., & Linder, E. V. 2010, *Phys. Rev. D*, 81, 103513
- Dent, J. B., Dutta, S., & Weiler, T. J. 2009, *Phys. Rev.*, D79, 023502
- Di Porto, C., Amendola, L., & Branchini, E. 2012, *Mon. Not. Roy. Astron. Soc.*, 419, 985
- Dossett, J., & Ishak, M. 2013, *Phys. Rev. D*, D88, 103008
- Efstathiou, G. 1999, *Mon. Not. Roy. Astron. Soc.*, 310, 842
- Eisenstein, D. J., et al. 2005, *ApJ*, 633, 560
- Elizalde, E., Nojiri, S., & Odintsov, S. D. 2004, *Phys. Rev.*, D70, 043539
- Erickson, J. K., Caldwell, R., Steinhardt, P. J., Armendariz-Picon, C., & Mukhanov, V. F. 2002, *Phys. Rev. Lett.*, 88, 121301
- Farooq, O., Madiyar, F. R., Crandall, S., & Ratra, B. 2017, *Astrophys. J.*, 835, 26
- Fay, S. 2016, arXiv:1605.01644
- Feng, C.-J., Shen, X.-Y., Li, P., & Li, X.-Z. 2012, *JCAP*, 1209, 023
- Frampton, P. H., & Ludwick, K. J. 2011, *Eur. Phys. J.*, C71, 1735
- Frieman, J., Turner, M., & Huterer, D. 2008, *Ann. Rev. Astron. Astrophys.*, 46, 385
- Fu, L., et al. 2008, *Astron. Astrophys.*, 479, 9
- Fu, X.-y., Wu, P.-x., & Yu, H.-w. 2009, *Phys. Lett.*, B677, 12
- Gannouji, R., Moraes, B., Mota, D. F., et al. 2010, *Phys. Rev.*, D82, 124006
- Gannouji, R., Moraes, B., & Polarski, D. 2009, *JCAP*, 0902, 034
- Garriga, J., & Mukhanov, V. F. 1999, *Phys. Lett.*, B458, 219
- Gaztanaga, E., Cabre, A., & Hui, L. 2009, *Mon. Not. Roy. Astron. Soc.*, 399, 1663
- Gong, Y. 2008, *Phys. Rev.*, D78, 123010
- Gruber, C., & Luongo, O. 2014, *Phys. Rev.*, D89, 103506
- Hinshaw, G., et al. 2013, *ApJS*, 208, 19
- Hu, W., & Scranton, R. 2004, *Phys. Rev. D*, 70, 123002
- Ishak, M., & Dossett, J. 2009, *Phys. Rev. D*, 80, 043004
- Jarosik, N., Bennett, C. L., Dunkley, J., et al. 2011, *ApJS*, 192, 14
- Jassal, H. K., Bagla, J. S., & Padmanabhan, T. 2005, *Mon. Not. Roy. Astron. Soc.*, 356, L11
- Koivisto, T., & Mota, D. F. 2007, *Phys. Lett.*, B644, 104
- Komatsu, E., Dunkley, J., Nolta, M. R., & et al. 2009, *ApJS*, 180, 330
- Komatsu, E., Smith, K. M., Dunkley, J., & et al. 2011, *ApJS*, 192, 18
- Kowalski, M., Rubin, D., Aldering, G., & et al. 2008, *ApJ*, 686, 749
- Li, J., Yang, R., & Chen, B. 2014, *JCAP*, 1412, 043
- Linder, E. V. 2003, *Phys. Rev. Lett.*, 90, 091301
- Linder, E. V., & Cahn, R. N. 2007, *Astroparticle Physics*, 28, 481
- Linder, E. V., & Jenkins, A. 2003, *Mon. Not. Roy. Astron. Soc.*, 346, 573
- Llinares, C., & Mota, D. 2013, *Phys. Rev. Lett.*, 110, 161101
- Llinares, C., Mota, D. F., & Winther, H. A. 2014, *Astron. Astrophys.*, 562, A78
- Lue, A., Scoccimarro, R., & Starkman, G. D. 2004, *Phys. Rev.*, D69, 124015
- Malekjani, M., Basilakos, S., Davari, Z., Mehrabi, A., & Rezaei, M. 2017, *Mon. Not. Roy. Astron. Soc.*, 464, 1192
- Malekjani, M., Naderi, T., & Pace, F. 2015, *Mon. Not. Roy. Astron. Soc.*, 453, 4148
- Maor, I., Brustein, R., & Steinhardt, P. J. 2001, *Phys. Rev. Lett.*, 86, 6, [Erratum: *Phys. Rev. Lett.*87,049901(2001)]
- Mehrabi, A., Basilakos, S., Malekjani, M., & Davari, Z. 2015a, *Phys. Rev.*, D92, 123513
- Mehrabi, A., Basilakos, S., & Pace, F. 2015b, *MNRAS*, 452, 2930
- Mehrabi, A., Malekjani, M., & Pace, F. 2015c, *Astrophys. Space Sci.*, 356, 129
- Mehrabi, A., Pace, F., Malekjani, M., & Del Popolo, A. 2017, *Mon. Not. Roy. Astron. Soc.*, 465(3), 2687
- Moresco, M., et al. 2012, *JCAP*, 1208, 006
- Mota, D. F., Kristiansen, J. R., Koivisto, T., & Groeneboom, N. E. 2007, *Mon. Not. Roy. Astron. Soc.*, 382, 793
- Mota, D. F., Sandstad, M., & Zlosnik, T. 2010, *JHEP*, 12, 051
- Mota, D. F., Shaw, D. J., & Silk, J. 2008, *Astrophys. J.*, 675, 29
- Naderi, T., Malekjani, M., & Pace, F. 2015, *MNRAS*, 447, 1873
- Nazari-Pooya, N., Malekjani, M., Pace, F., & Jassur, D. M.-Z. 2016, *Mon. Not. Roy. Astron. Soc.*, 458, 3795
- Nesseris, S., Blake, C., Davis, T., & Parkinson, D. 2011, *JCAP*, 1107, 037
- Nesseris, S., & Perivolaropoulos, L. 2008, *Phys. Rev.*, D77, 023504
- Nesseris, S., & Sapone, D. 2014, ArXiv e-prints, 1409.3697, arXiv:1409.3697
- Pace, F., Batista, R. C., & Popolo, A. D. 2014a, *MNRAS*, 445, 648
- Pace, F., Batista, R. C., & Del Popolo, A. 2014b, *MNRAS*, 445, 648
- Pace, F., Fedeli, C., Moscardini, L., & Bartelmann, M. 2012, *MNRAS*, 422, 1186
- Pace, F., Moscardini, L., Crittenden, R., Bartelmann, M., & Pettorino, V. 2014c, *Mon. Not. Roy. Astron. Soc.*, 437, 547
- Pace, F., Waizmann, J. C., & Bartelmann, M. 2010, *MNRAS*, 406, 1865
- Pade, H. 1892, *Ann. Sci. Ecole Norm. Sup.*, 9(3), 1
- Padmanabhan, N., Xu, X., Eisenstein, D. J., et al. 2012, *MNRAS*, 427, 2132
- Padmanabhan, T. 2002, *Phys. Rev. D*, 66, 021301
- . 2003, *PhR*, 380, 235
- Peebles, P. J., & Ratra, B. 2003, *Reviews of Modern Physics*, 75, 559
- Peebles, P. J. E. 1993, *Principles of physical cosmology* (Princeton University Press)
- Percival, W. J., Reid, B. A., Eisenstein, D. J., & et al. 2010, *MNRAS*, 401, 2148
- Perlmutter, S., Aldering, G., Goldhaber, G., & et al. 1999, *ApJ*, 517, 565
- Planck Collaboration XIV. 2016, *Astron. Astrophys.*, 594, A14
- Polarski, D., & Gannouji, R. 2008, *Physics Letters B*, 660, 439
- Reid, B. A., Samushia, L., White, M., et al. 2012, *MNRAS*, 426, 2719
- Riess, A. G., Filippenko, A. V., Challis, P., & et al. 1998, *AJ*, 116, 1009
- Riess, A. G., et al. 2004, *ApJ*, 607, 665
- Sahni, V., & Starobinsky, A. A. 2000, *IJMPD*, 9, 373
- Sapone, D., & Majerotto, E. 2012, *Phys. Rev. D*, 85, 123529
- Schwarz, G. 1978, *Ann. Stat.*, 6, 461
- Seljak, U., et al. 2005, *Phys. Rev.*, D71, 103515
- Serra, P., Cooray, A., Holz, D. E., et al. 2009, *Phys. Rev. D*, 80, 121302
- Silveira, V., & Waga, I. 1994, *Phys. Rev.*, D50, 4890
- Steigerwald, H., Bel, J., & Marinoni, C. 2014, *JCAP*, 1405, 042
- Suzuki, N., Rubin, D., Lidman, C., Aldering, G., & et al. 2012, *ApJ*, 746, 85

- Taddei, L., & Amendola, L. 2015, JCAP, 1502, 001
- Tegmark, M., et al. 2004, Phys. Rev. D, 69, 103501
- Tsujikawa, S., Gannouji, R., Moraes, B., & Polarski, D. 2009, Phys. Rev., D80, 084044
- Wang, L., & Steinhardt, P. J. 1998a, ApJ, 508, 483
- Wang, L.-M., & Steinhardt, P. J. 1998b, Astrophys. J., 508, 483
- Wei, H. 2008, Phys. Lett., B664, 1
- Wei, H., Yan, X.-P., & Zhou, Y.-N. 2014, JCAP, 1401, 045
- Weinberg, D. H., Mortonson, M. J., Eisenstein, D. J., et al. 2013, Phys. Rept., 530, 87
- Weinberg, S. 1989, Reviews of Modern Physics, 61, 1
- Wetterich, C. 2004, Phys. Lett., B594, 17
- Wu, P., Yu, H. W., & Fu, X. 2009, JCAP, 0906, 019
- Yang, W., Xu, L., Wang, Y., & Wu, Y. 2014, Phys. Rev., D89, 043511
- Zaninetti, L. 2016, Submitted to: Galaxies, arXiv:1602.06418
- Zhou, Y.-N., Liu, D.-Z., Zou, X.-B., & Wei, H. 2016, Eur. Phys. J., C76, 281